2016 13th International Conference on Ubiquitous Robots and Ambient Intelligence (URAI)
August 19~22, 2016 at Sofitel Xian on Renmin Square, Xian, China

Adaptive Inverse Perspective Mapping for Lane Map Generation with SLAM

Jinyong Jeong and Ayoung Kim[1]
[1]Department of Civil and Environmental Engineering, KAIST, S. Korea
(Tel : +82-042-350-3672; E-mail: [jjy0923, ayoungk]@kaist.ac.kr)

***Abstract*—This paper proposes an adaptive Inverse Perspective Mapping (IPM) algorithm to obtain accurate bird's-eye view images from the sequential images of forward looking cameras. These images are often distorted by the motion of the vehicle; even a small motion can cause a substantial effect on bird's-eye view images. In this paper, we propose an adaptive model for the IPM to accurately transform camera images to bird's-eye view images by using motion information. Using motion derived from the monocular visual simultaneous localization and mapping (SLAM), experimental result shows that the proposed approaches can provide stable bird's-eye view images, even with large motion during the drive.**

***Keywords*—Adaptive Inverse Perspective Mapping, Monocular Visual SLAM, Ego Motion Estimation**

1. Introduction

The intelligent transportation system has recently been highlighted by many research studies. One popular intelligent transportation system, the Advanced Driver Assistance Systems (ADAS), is considered an important subject because it has a significant impact on people's safety. One of the important features of the ADAS system is the perception of road and lane, which aims to understand the environment that surrounds the vehicle. This paper focuses on a mathematical technique called IPM that is often used in vision based perception of roads and lanes. IPM produces bird's-eye view images that remove perspective effect by using information about camera parameters and the relationship between the camera and the ground. The results of IPM can provide post-algorithms with more efficient information, such as lane perception, mapping, localization and pattern recognition.

Many researchers have studied IPM in many applications, such as distance detection[1], the production of bird's-eye view images of the spacious area by using a mosaic method[2], the provision of appropriate bird's-eye view images for parking assistance[3], and lane-level map generation[4]. Conventional IPM assumes a rigid body relationship between the camera and the ground. However, when a moving platform undergoes severe change in motion, this assumption breaks and the bird's-eye view is warped by the motion. In this paper, we propose an extended IPM model that can compute accurate bird's-eye view images under the camera motion. A mono visual odometry algorithm is also used to calculate the motion of the camera.

The paper is organized as follows. §2 presents the adaptive IPM model that we proposed, experiment results are given in §3, finally, the conclusion is presented in §4.

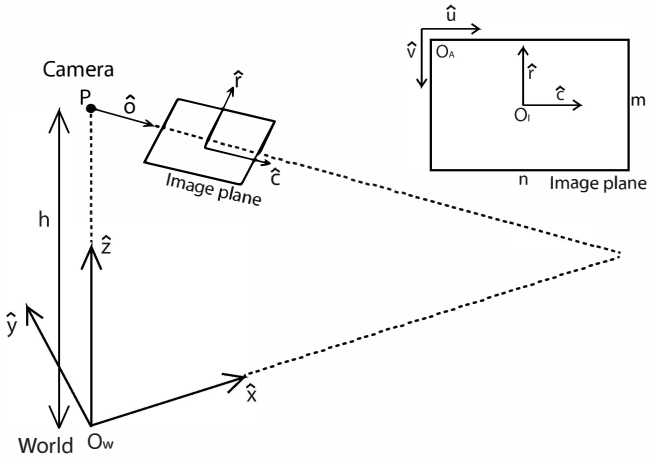

Fig. 1. Coordinate the relationship between the camera, image and world. The unit of $(\hat{u}, \hat{v})$ is the pixel measurement, and that of $(\hat{r}, \hat{c})$ and $(\hat{X}, \hat{Y}, \hat{Z})$ is the meter measurement.

2. The Adaptive IPM Model

We first describe the basic IPM model [5] by using physical parameters of a camera before illustrating an adaptive IPM model. IPM is a mathematical technique that relates to coordinate systems with different perspectives. For example, this method can be applied in order to obtain undisturbed bird's-eye view images given forward-facing distorted images. Fig. 1 illustrates the relationship of coordinate systems between the camera, image and world.

Using IPM we aim to map pixel points (u, v) to world coordinate points (X, Y, Z). The notation $(\hat{\cdot})$ indicates a vectored version of the variables. We first define a unit vector $\hat{X}$ to set the camera's viewing direction. Being orthogonal to $\hat{X}$, we define another unit vector ,$\hat{Y}$, that is orthogonal to both ground and the camera-viewing direction.

The IPM is to find the relation between the world coordinate $(\hat{X}, \hat{Y}, \hat{Z})$ and image coordinate $(\hat{u}, \hat{v})$ in order to map image pixels to world coordinate points. Note that two types of coordinates on an image are set as $(\hat{u}, \hat{v})$ and $(\hat{r}, \hat{c})$, depending on the unit. The relation between an image point in a pixel space $(\hat{u}, \hat{v})$ and the same point in a meter space $(\hat{r}, \hat{c})$ is defined as below.

$$\mathbf{u}(\mathbf{c}) = \frac{\mathbf{n}+1}{2} + \mathbf{K}\mathbf{c} \quad \longleftrightarrow \quad \mathbf{c}(\mathbf{u}) = \frac{1}{\mathbf{K}}(\mathbf{u} - \frac{\mathbf{n}+1}{2}) \quad (1)$$

$$\mathbf{v}(\mathbf{r}) = \frac{\mathbf{m}+1}{2} - \mathbf{K}\mathbf{r} \quad \longleftrightarrow \quad \mathbf{r}(\mathbf{v}) = \frac{1}{\mathbf{K}}(\frac{\mathbf{m}+1}{2} - \mathbf{v}) \quad (2)$$

978-1-5090-0821-6/16/$31.00 ©2016 IEEE

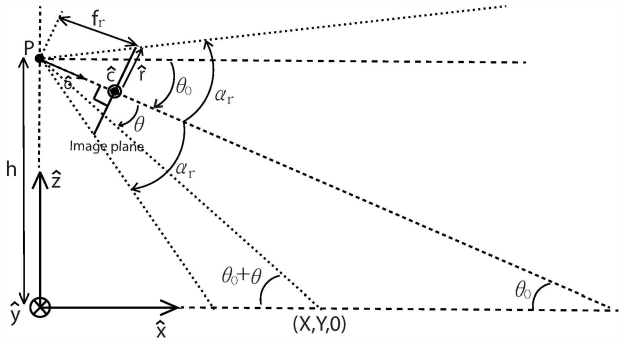

Fig. 2. Side view of IPM model.

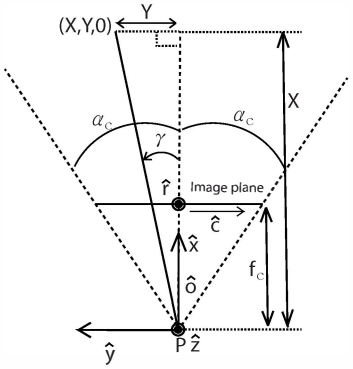

Fig. 3. Top view of IPM model.

with a scale factor between pixel and meter ($\mathrm{px/m}$) $\mathbf{K}$, the image width $\mathbf{m}$, and the images height $\mathbf{n}$. The location of the camera's optical center ($\mathbf{P}$) is $[0, 0, h]$ in the world coordinate system. The unit vector of the optical axis $\hat{o}$ is orthogonal to the image plane.

We further describe parameters via the side and top views as shown in Fig. 2 and Fig. 3. The projected images in the world coordinates can be calculated easily by assuming that the height of the objects is zero. Using the side view, a point X in $\hat{X}$ direction can be written as a function of pixel point v, a tilt angle of a camera (θ_0) and a vertical angle (θ).

$$\mathbf{X}(\mathbf{v}) \quad = \quad \mathbf{h}\cot(\theta_0 + \theta(v)) \tag{3}$$

The tilt angle stands for an angle between a line that is parallel to the ground and an optical axis ($\hat{o}$); the vertical angle is the angle between a line from $\mathbf{P}$ to each pixel and $\hat{o}$. Using geometry in Fig. 2, we now derive the tilt and vertical angle as a function of other image parameters. In finding this relation, we start from vertical focal length ($\mathbf{f_r}$) from which we can directly inform $\theta(v)$ via $\theta(v) = \arctan(\frac{\mathbf{r(v)}}{\mathbf{f_r}})$. By applying geometry, we find an equation for $\mathbf{f_r}$ as a function of $\mathbf{r}_{top}$ and $\tan(\alpha_r)$.

$$\tan(\alpha_r) \quad = \quad \frac{\mathbf{r}_{top}}{\mathbf{f_r}} \tag{4}$$

$\mathbf{r}_{top}$ is the $\mathbf{r}$ value of the highest point in ($\hat{r}$, $\hat{c}$) coordinate and α_r is the half angle of the vertical field of view (FOV). The $\mathbf{r}_{top}$ value can be derived when the value of v is 1.

$$\mathbf{r}_{top} \quad = \quad \mathbf{r}(\mathbf{v}=1) = \frac{1}{\mathbf{K}}\frac{\mathbf{m}-1}{2} \tag{5}$$

Then $\mathbf{f_r}$ can be derived using (4) and (5).

$$\mathbf{f_r} \quad = \quad \mathbf{r}_{top}\cot(\alpha_r) = \frac{\mathbf{m}-1}{\mathbf{2K}}\cot(\alpha_r) \tag{6}$$

Using (6), $\theta(\mathbf{v})$ can be written as

$$\begin{aligned}\theta(\mathbf{v}) &= \arctan\Big(\frac{\mathbf{r(v)}}{\mathbf{f_r}}\Big) \\ &= \arctan\Big(\Big(\mathbf{1} - 2\frac{\mathbf{v}-\mathbf{1}}{\mathbf{m}-\mathbf{1}}\Big)\tan(\alpha_r)\Big).\end{aligned} \tag{7}$$

Finally, we can get a formula of $\mathbf{X}(\mathbf{v})$ using (7).

$$\begin{aligned}\mathbf{X}(\mathbf{v}) &= \mathbf{h}\cot(\theta_0 + \theta(v)) \\ &= \mathbf{h}\frac{\tan(\theta_0)\tan(\theta(\mathbf{v})) - \mathbf{1}}{\tan(\theta_0) + \tan(\theta(\mathbf{v}))} \\ &= \mathbf{h}\frac{\tan(\theta_0)\Big(\mathbf{1} - 2\frac{\mathbf{v}-\mathbf{1}}{\mathbf{m}-\mathbf{1}}\Big)\tan(\alpha_r) - \mathbf{1}}{\tan(\theta_0) + \Big(\mathbf{1} - 2\frac{\mathbf{v}-\mathbf{1}}{\mathbf{m}-\mathbf{1}}\Big)\tan(\alpha_r)}\end{aligned} \tag{8}$$

Note that $\mathbf{X}$ in the world coordinate is independent on the $\mathbf{u}$ of the image plane.

Next we derive $\mathbf{Y}$ by using top view as in Fig. 3. This relation can be derived using a proportional expression between $\mathbf{X}$ and $\mathbf{Y}$.

$$\frac{\mathbf{Y}(\mathbf{u},\mathbf{v})}{\mathbf{X}(\mathbf{v})} \quad = \quad -\frac{\mathbf{c}}{\mathbf{f_c}} \tag{9}$$

, where $\mathbf{f_c}$ is the horizontal focal length, which can be obtained from

$$tan(\alpha_c) = \frac{\mathbf{c}_{right}}{\mathbf{f_c}} \tag{10}$$

Similar to the side view geometry, $\mathbf{c}_{right}$ is the $\mathbf{c}$ value of the far right point in ($\hat{r}$, $\hat{c}$) coordinate and α_c is the half angle of horizontal FOV. $\mathbf{c}_{right}$ can be obtained when the u value is n.

$$\mathbf{c}_{right} \quad = \quad \mathbf{c}(\mathbf{u}=\mathbf{n}) = \frac{\mathbf{1}}{\mathbf{K}}\Big(\frac{\mathbf{n}-\mathbf{1}}{\mathbf{2}}\Big) \tag{11}$$

Therefore, $\mathbf{f_c}$ and $\mathbf{Y}(\mathbf{u},\mathbf{v})$ can be defined as (12), (13). If the width and height of the image is the same ($m = n$), then $\mathbf{f_c}$ is the same as $\mathbf{f_r}$.

$$\mathbf{f_c} \quad = \quad \frac{\mathbf{c}_{right}}{tan(\alpha_c)} = \frac{\mathbf{n}-\mathbf{1}}{\mathbf{2K}\tan(\alpha_c)} \tag{12}$$

$$\begin{aligned}\mathbf{Y}(\mathbf{u},\mathbf{v}) &= -\frac{\mathbf{1}}{\mathbf{K}}\Big(\mathbf{u} - \frac{\mathbf{n}+\mathbf{1}}{\mathbf{2}}\Big)\frac{\mathbf{2K}\tan(\alpha_c)}{\mathbf{n}-\mathbf{1}}\mathbf{X}(\mathbf{v}) \\ &= \Big(\mathbf{1} - \mathbf{2}\frac{\mathbf{u}-\mathbf{1}}{\mathbf{n}-\mathbf{1}}\Big)\tan(\alpha_c)\mathbf{X}(\mathbf{v})\end{aligned} \tag{13}$$

The location of $\mathbf{Y}(\mathbf{u},\mathbf{v})$ in the world coordinate is dependent on $(\mathbf{u},\mathbf{v})$ because $\mathbf{Y}(\mathbf{u},\mathbf{v})$ includes $\mathbf{X}(\mathbf{v})$. But this model only considers a case getting images from a fixed camera. When images are obtained from a moving vehicle, it is difficult

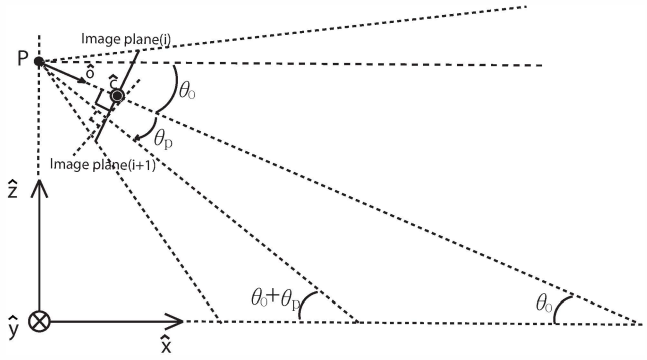

Fig. 4. Side view of the adaptive IPM model. The pitch angle of a camera (θ_p) is added to the basic IPM model.

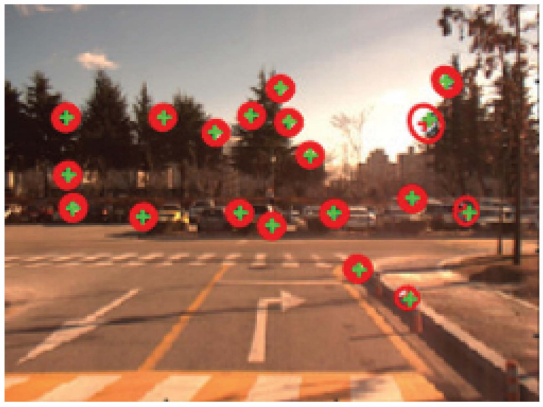

Fig. 5. Feature points derived from visual odometry. The motions of a camera (x, y, z, roll, pitch, yaw) can be calculated using this algorithm.

for them to be transformed to the accurate bird's-eye view images because of the motion of the vehicle, especially its pitch direction. To solve this problem, an angle in the pitch direction (θ_p) of the camera is also added in this model, as illustrated in Fig. 4.

Finally, the adaptive IPM modeling equations (14) can be derived by adding θ_p to original θ_0.

$$\begin{aligned} \mathbf{X}(\mathbf{v}, \theta_\mathbf{p}) &= \mathbf{h}\frac{\tan(\theta_0+\theta_p)\left(\mathbf{1}-2\frac{\mathbf{v}-\mathbf{1}}{\mathbf{m}-\mathbf{1}}\right)\tan(\alpha_r)-\mathbf{1}}{\tan(\theta_0+\theta_p)+\left(\mathbf{1}-2\frac{\mathbf{v}-\mathbf{1}}{\mathbf{m}-\mathbf{1}}\right)\tan(\alpha_r)} \\ \mathbf{Y}(\mathbf{u}, \mathbf{v}, \theta_\mathbf{p}) &= \left(\mathbf{1}-\mathbf{2}\frac{\mathbf{u}-\mathbf{1}}{\mathbf{n}-\mathbf{1}}\right)\tan(\alpha_c)\mathbf{X}(\mathbf{v}, \theta_\mathbf{p}) \end{aligned} \quad (14)$$

$\mathbf{X}(\mathbf{v}, \theta_\mathbf{p})$ is dependent on the pitch angle of the camera (θ_p) and $\mathbf{Y}(\mathbf{u}, \mathbf{v}, \theta_\mathbf{p})$ is also dependent on it, which means that bird's-eye view images are properly compensated against the pitch angle.

3. Experimental Results

The performance of the adaptive IPM model has been tested on real image sequences acquired on the Korea Advanced Institute of Science & Technology (KAIST) campus with a forward-facing camera mounted on a vehicle. The testing images have a resolution of $\mathbf{1280 \times 960}$ and were captured at 15 **fps**. We use the mono visual odometry algorithm [6][7] to obtain the vehicle motion. Fig. 5 shows the feature points that were obtained by this method.

Fig. 6 and Fig. 7 show comparisons between the results of the existing IPM model and the adaptive IPM model when the vehicle on which the camera is mounted encounters a speed bump. In Fig. 6, the pitch angle is changed around 4.1 degrees from Fig. 6(a) to Fig. 6(c). Fig. 6(c) shows the result of the existing IPM model. The bird's-eye view image of this model is distorted because of image change due to vehicle's motion. On the other hand, the result of the adaptive IPM (Fig. 6(d)) model shows an undistorted bird's-eye view image despite the vehicle motion.

In Fig. 7, the pitch angle is changed around 2.1 degrees from Fig. 7(a) to Fig. 7(c). An angle change of approximately 2.1 degrees is a considerably small motion, but it can substantially distort a bird's eye view image as depicted in Fig. 7(c). Fig. 7(d) shows an undistorted bird's-eye view image using the adaptive IPM model.

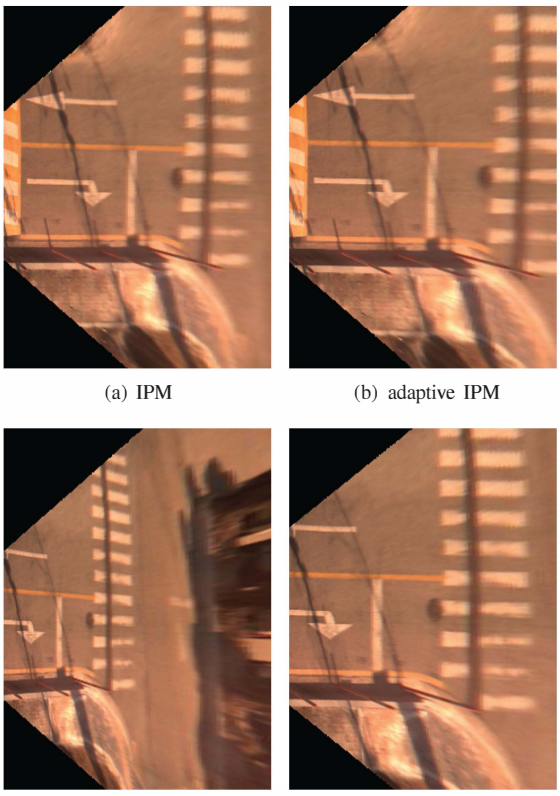

(a) IPM (b) adaptive IPM

(c) IPM (after 7 frame) (d) adaptive IPM (after 7 frame)

Fig. 6. Experimental results of the data set 1 having a speed bump. There is about 4.1 degrees of difference in the pitch angle between image (**a**) and (**c**). (**c**) and (**d**) are 7 frames after (**a**) and (**b**).

4. Conclusion

We propose an adaptive IPM model that consider the motion, especially the pitch angle which is paramount of the

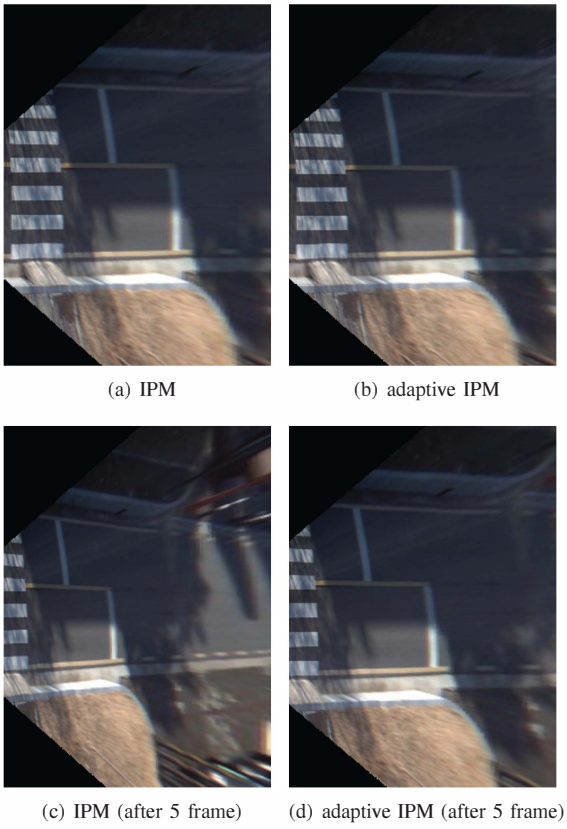

(a) IPM (b) adaptive IPM

(c) IPM (after 5 frame) (d) adaptive IPM (after 5 frame)

Fig. 7. Experimental results of data set 2 having a speed bump. There is about 2.1 degrees of difference in pitch angle between image (**a**) and (**c**). (**c**) and (**d**) are 5 frames after (**a**) and (**b**).

vehicle mounting the camera. Our model has been verified in a situation that involved a significant change in the pitch angle when the vehicle passes speed bumps, and the compensation result that pertains to such a motion's impact on bird's eye view images is checked. The results that employ the adaptive IPM model can be provided to other algorithms, such as those involving lane detection and the perception of obstacles to obtain more accurate performance.

Motion of the pitch is only considered in this model, so there is a small amount of distortion in bird's-eye view images because of the roll motion. Thus, our model can be improved by adding a roll parameter to obtain a more robust IPM model against the motion of the camera.

ACKNOWLEDGEMENT

This work is supported through a grant from the Korea Evaluation Institute of Industrial Technology (KEIT) (Award #N02150031) and KAIST Institute for Robotics and u-city program by Ministry of Land, Infrastructure, and Transport, Korea.

REFERENCES

[1] Shane Tuohy, D OCualain, E Jones, and M Glavin. Distance determination for an automobile environment using inverse perspective mapping in opencv. In *Proc. Irish Signals and Systems Conference*, volume 2010, 2010.

[2] Robert Laganiere. Compositing a birds eye view mosaic. In *Proc. Conf. Vision Interface*, pages 382–387. Citeseer, 2000.

[3] Chien-Chuan Lin and Ming-Shi Wang. A vision based top-view transformation model for a vehicle parking assistant. *Sensors*, 12(4):4431–4446, 2012.

[4] Chunzhao Guo, Jun-ichi Meguro, Yasuhiro Kojima, and Tomoyuki Naito. Automatic lane-level map generation for advanced driver assistance systems using low-cost sensors. In *Robotics and Automation (ICRA), 2014 IEEE International Conference on*, pages 3975–3982. IEEE, 2014.

[5] Hanspeter A Mallot, Heinrich H Bülthoff, JJ Little, and Stefan Bohrer. Inverse perspective mapping simplifies optical flow computation and obstacle detection. *Biological cybernetics*, 64(3):177–185, 1991.

[6] J. Civera, A.J. Davison, and J. Montiel. Inverse depth parametrization for monocular slam. *IEEE Transaction on Robotics*, 24(5):932–945, Oct. 2008.

[7] Javier Civera, Oscar G Grasa, Andrew J Davison, and JMM Montiel. 1-point ransac for extended kalman filtering: Application to real-time structure from motion and visual odometry. *Journal of Field Robotics*, 27(5):609–631, 2010.